Int. J. Heat Mass Transfer. Vol. 28, No. 11, pp. 2029–2041, 1985
Printed in Great Britain

0017–9310/85 $3.00 + 0.00

Two-dimensional buoyant plume in porous media: higher-order effects

NOOR AFZAL
Department of Mechanical Engineering, Aligarh Muslim University, Aligarh—202001, India

(*Received* 8 *October* 1984)

Abstract—The natural convection from a two-dimensional horizontal line source of heat embedded in a porous media has been studied by the method of matched asymptotic expansions at large Rayleigh numbers. The general case of a confined plume emerging from the apex of an insulated symmetric wedge with its axis coinciding with the direction of buoyant force vector is considered for arbitrary values of wedge angles. The first-order problem reduces to the boundary-layer approximation considered earlier by Wooding [*J. Fluid Mech.* **15**, 527–544 (1963)]. For the second-order boundary layer equations, representing the entrainment effect, a closed-form solution is given and for the third-order equations representing the effects of axial heat conduction and normal pressure gradiant the equations are integrated numerically. The results are displayed graphically and discussed critically.

1. INTRODUCTION

THE IMPETUS for the development of alternate energy sources and utilization of geothermal energy has led to increasing research activities on the natural convection in porous media. The reviews on the available literature may be found in the works of Cambarnous and Boris [1] and Cheng [2].

The problem of a plume arising from a horizontal line source of heat in a porous media was first considered by Wooding [3]. By employing classical boundary-layer theory to the equations for Darcian flow in a porous media, Wooding [3] noted that the resulting equations are analogous to that of Schlichting's two-dimensional jet in a Newtonian fluid, and a closed-form solution was presented when the Prandtl number is unity. Yih [4] later pointed out that the solution of Wooding [3] is actually valid for all Prandtl numbers.

The solution of Wooding [3] based on the classical boundary-layer approximation is valid for large values of Rayleigh numbers; it neglects the conduction in axial direction, normal pressure gradient and the entrainment in the plume from the outer region. For geothermal systems the Rayleigh numbers, of the order of 300–1000 [2], are not very large. Therefore, from point of view of applications it would be of great interest to refine the boundary-layer analysis [3] to include the higher-order effects so that the results can be utilized for low or moderate values of Rayleigh numbers.

Based on the method of matched asymptotic expansions, the higher-order effects to Prandtl's boundary layer in a Newtonian fluid had been studied by several workers [5]. The higher-order boundary layer for natural convection on a vertical plate was first studied by Yang and Jerger [6]. Riley [7] as well as Hieber and Nash [8] have studied higher-order effects for free convection arising from a horizontal source of heat in a Newtonian fluid [9]. The higher-order effects in Darcian natural convection flow from horizontal plates has been studied by Chang and Cheng [10].

The present work deals with the study of higher-order effects in natural convection flow arising from a two-dimensional horizontal line source of heat embedded in Darcian porous media. The general case of a confined plume emerging from the apex of an insulated symmetric wedge of angle 2β with its axis coinciding with the direction of buoyant force vector (see Fig. 1) is considered. The special case of $\beta = \pi$ corresponds to a free plume in an infinite expanse of porous media and $\beta = \pi/2$ corresponds to the plume bounded by a horizontal insulated surface. At large values of Rayleigh number the flow field is divided into two layers: inner and outer. In the inner layer, in the neighbourhood of the plane of symmetry, the convection and conduction terms in the energy equation are of the same order and axial velocity is governed by local buoyancy. In the outer layer, away from the plane of symmetry, conductive transport is negligible. The asymptotic expansions in the inner and outer regions are matched in the overlap domain. The

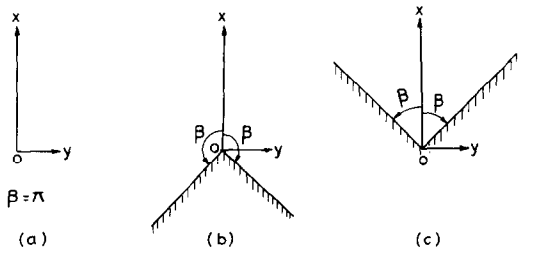

FIG. 1. Coordinate system for the plume where horizontal line heat source is situated at point 0 in a Darcian porous media. (a) Free or unbounded plume; (b) and (c) plume bounded by two adiabatic inclined plates forming a symmetrical wedge of included angle 2β.

NOMENCLATURE

$A_0, A_1, A_2, \ldots$ constants
C unspecified eigenconstant
C_p specific heat
f_0, f_1, f_2 first-, second- and third-order stream functions in the inner layer
F_m eigenvector for velocity distribution in the inner layer
g gravitational acceleration
h_0, h_1, h_2 first-, second- and third-order temperatures in the inner layer
H_m eigenvector for temperature distribution in the inner layer
k_m eigenvalue in the outer layer
K permeability of porous media
L characteristic length
Q rate of heat released from point source
Ra Rayleigh number defined by equation (9)
Ra_x local Rayleigh number defined by equation (95)
t temperature in inner layer defined by equation (23)
t_0, t_1, t_2 first-, second- and third-order temperatures in inner layer defined by expansion (28b)
$\tilde{t}_m$ eigenvector for temperature in the inner layer defined by expansion (28b)
T non-dimensional temperature defined by equation (7)
W complex velocity potential defined by $W(Z) = \Phi(X, Y) + i\Psi(X, Y)$
W_1, W_2, W_3 first-, second- and third-order complex potential in the outer layer
$\tilde{W}_m$ eigensolution for complex potential in outer layer
T_0, T_1, T_2 first-, second- and third-order temperatures in the outer layer defined by expansion (16b)
x vertical coordinate measured from the heat source in the inner layer
X non-dimensional vertical coordinate ($X = x$)
y stretched normal coordinate in the inner layer defined by equation (23)
Y non-dimensional normal coordinate
Z a complex variable, $Z = X + iY$

Greek symbols

α thermal diffusivity
α_m eigenvalues in the inner layer defined by equation (48)
β half the angle of the insulated wedge (bounding the porous media) measured from the axis of the wedge (Fig. 1)
γ volumetric thermal expansion coefficient
δ half-width of plume defined by equation (92)
ε appropriate perturbation parameter, $Ra_x^{-1/3}$
η similarity variable defined by equations (41) or (92)
θ angular coordinate measured from the axis of wedge
θ_T characteristic temperature defined by equation (8b)
λ perturbation parameter defined by equation (15)
μ molecular viscosity of the fluid
ρ density of fluid
ψ stream function in inner layer defined by equation (23)
ψ_0, ψ_1, ψ_2 first-, second- and third-order stream functions in inner layer defined by equation (28a)
Ψ non-dimensional stream function defined by equation (7)
Ψ_0, Ψ_1, Ψ_2 first-, second- and third-order stream functions in outer layer defined by equation (16a)
$\tilde{\Psi}_m$ eigenvector for stream function in the outer layer defined by equation (16a).

small parameter is the inverse cube root of the appropriate Rayleigh number based on the amount of heat released from the source and the permeability of the porous media. The leading term in the expansions represent the boundary-layer approximation of Wooding [3] and higher-order perturbations represent the corrections required at moderately large values of Rayleigh number. The second-order boundary-layer equations account for the entrainment of outer irrotational fluid in the boundary layer, which is known as the displacement effect. The third-order boundary-layer equations take into consideration the effects of streamwise heat conduction and transverse pressure gradient. The first eigensolution associated with the problem arises with the fourth-order boundary-layer equations. In the inner layer the various order equations admit self-similarity. For the first- and second-order boundary-layer equations closed-form solutions are presented and the third-order boundary-layer equations are solved numerically.

2. ANALYSIS

The equations governing the buoyancy-induced motion arising from a horizontal line source of heat for a Darcian flow in a porous media with Boussinesq approximation are [2]

$$\frac{\partial^2 \Psi_*}{\partial X_*^2} + \frac{\partial^2 \Psi_*}{\partial Y_*^2} = \frac{g\gamma K}{\nu} \frac{\partial T_*}{\partial Y_*} \tag{1}$$

$$\frac{\partial \Psi_*}{\partial Y_*} \frac{\partial T_*}{\partial X_*} - \frac{\partial \Psi_*}{\partial X_*} \frac{\partial T_*}{\partial Y_*} = \alpha \left(\frac{\partial^2 T_*}{\partial X_*^2} + \frac{\partial^2 T_*}{\partial Y_*^2} \right) \tag{2}$$

where X_* and Y_* are the coordinates along the buoyant force vector measured from heat source and normal to it, γ is the volumetric expansion coefficient, g is the gravitational acceleration, K is the permeability of porous media, $\nu = \mu/\rho$ is the molecular kinematic viscosity of the fluid, μ is the dynamic viscosity, ρ is the density of the fluid and α is the thermal diffusivity of the fluid. Further, T_* is the temperature and Ψ_* is the stream function defined by

$$U_* = \frac{\partial \Psi_*}{\partial Y_*}, \quad V_* = -\frac{\partial \Psi_*}{\partial X_*}$$

where U_* and V_* are the velocity components in X_* and Y_* directions, respectively.

The boundary conditions at the axis of the plume are that of symmetry with respect to the X_* axis

$$X_* > 0, \quad Y_* = 0: \quad \Psi_* = \frac{\partial^2 \Psi_*}{\partial Y_*^2} = \frac{\partial T_*}{\partial Y_*} = 0. \tag{3}$$

The boundary conditions for confined plume (Fig. 1) emerging from the apex of an insulated symmetric wedge of angle 2β with its axis $\theta = 0$ coinciding with the direction of the buoyant force vector are

$$\theta = \pm\beta, \quad \Psi_* = \text{grad } T_* = 0 \tag{4}$$

where θ is given by

$$\theta = \tan^{-1}(Y_*/X_*).$$

Far away from the heat source the velocity and temperature approach their ambient value

$$\begin{aligned} &-\beta < \theta < \beta, \quad X_*^2 + Y_*^2 \to \infty; \\ &\frac{\partial \Psi_*}{\partial Y_*} \to 0, \quad T_* \to T_{*\infty}. \end{aligned} \tag{5}$$

For a large control volume enclosing the heat source, integration of energy equation (2) leads to

$$\frac{Q}{\rho C_p} = \int_0^\infty \frac{\partial \Psi_*}{\partial Y_*} (T_* - T_{*\infty}) \, dY_* - \alpha \int_{-\infty}^{\infty} \frac{\partial T_*}{\partial X_*} dY_* \tag{6}$$

where Q is the heat released by the horizontal line source of heat.

We consider the following non-dimensional variables

$$\begin{aligned} &X_* = XL, \quad Y_* = YL \\ &\Psi_* = U_c L \Psi, \quad T_* - T_{*\infty} = \theta_T T \end{aligned} \tag{7}$$

where L is some reference length, U_c is the characteristic free convection velocity associated with the source in the porous media as

$$U_c = g\gamma K \theta_T / \nu \tag{8a}$$

and θ_T is the characteristic temperature difference associated with the heat source in porous media and based on relation (6) it can be adopted as

$$\theta_T = \left[\left(\frac{Q}{\rho C_p} \right)^2 \frac{\nu}{g\gamma KL\alpha} \right]^{1/3}. \tag{8b}$$

The appropriate Rayleigh number

$$Ra = \frac{Qg\gamma KL}{\rho C_p \nu \alpha^2} \tag{9}$$

is regarded as large. In terms of Ra the expressions (8a) and (8b) become

$$U_c L = \alpha Ra^{2/3} \tag{10a}$$

$$\theta_T = \frac{\nu\alpha}{g\gamma KL} Ra^{2/3} \tag{10b}$$

Based on non-dimensional variables (7), (9) and (10) the governing equations (1) and (2) become

$$\frac{\partial^2 \Psi}{\partial X^2} + \frac{\partial^2 \Psi}{\partial Y^2} = \frac{\partial T}{\partial Y} \tag{11}$$

$$\frac{\partial \Psi}{\partial Y} \frac{\partial T}{\partial X} - \frac{\partial \Psi}{\partial X} \frac{\partial T}{\partial Y} = \lambda^2 \left(\frac{\partial^2 T}{\partial X^2} + \frac{\partial^2 T}{\partial Y^2} \right). \tag{12}$$

The boundary conditions are

$$\begin{aligned} &X > 0, \quad Y = 0: \quad \Psi = \frac{\partial^2 \Psi}{\partial Y^2} = \frac{\partial T}{\partial Y} = 0 \\ &\theta = \pm\beta, \quad \Psi = \text{grad } T = 0 \\ &-\beta < \theta < \beta, \quad X^2 + Y^2 \to \infty, \quad \frac{\partial \Psi}{\partial Y} = T = 0 \end{aligned} \tag{13}$$

subject to the heat flux relation

$$\int_{-\infty}^{\infty} \frac{\partial \Psi}{\partial Y} T \, dY = \lambda + \lambda^2 \int_{-\infty}^{\infty} \frac{\partial T}{\partial X} dY. \tag{14}$$

Here λ is a parameter defined as

$$\lambda = Ra^{-1/3}. \tag{15}$$

For large values of Rayleigh number, the parameter λ can be taken as a small perturbation parameter. The outer expansions for stream function Ψ and temperature T are straightforward in the powers of λ as

$$\left.\begin{aligned} \Psi &= \Psi_0(X, Y) + \lambda\Psi_1(X, Y) + \lambda^2\Psi_2(X, Y) \\ &\quad + \cdots + \lambda^{k_m}\tilde{\Psi}_m(X, Y) + \cdots \\ T &= T_0(X, Y) + \lambda T_1(X, Y) + \lambda^2 T_2(X, Y) \\ &\quad + \cdots + \lambda^{k_m}\tilde{T}_m(X, Y) + \cdots \end{aligned}\right\} \tag{16}$$

where $\tilde{\Psi}_m$, $\tilde{T}_m$ are the eigensolution and k_ms the eigenvalues associated with the outer layer.

Substituting the outer expansions in equations (11) and (12) and collecting the coefficients of like powers of

λ we get equations for successive approximations

$$\nabla^2\Psi_n = T_{n,Y} \tag{17a}$$

$$\Psi_{0,Y}T_{n,x}-\Psi_{0,x}T_{n,Y} = a_{n-1}\sum_{j=0}^{n-1}(\Psi_{n-j+1,x}T_{j,Y} - \Psi_{n-j+1,Y}T_{j,x})+a_{n-2}\nabla^2 T_{n-2} \tag{17b}$$

where

$$\begin{aligned} a_n &= 0 \quad \text{for} \quad n<0 \\ &= 1 \quad \text{for} \quad n \geqslant 0. \end{aligned} \tag{18}$$

The boundary conditions are

$$-\beta<\theta<\beta, \quad Y\to\infty, \quad \Psi_{n,Y} = T_n = 0 \tag{19a}$$

$$\theta = \pm\beta, \quad \Psi_n = \text{grad } T_n = 0 \tag{19b}$$

$X>0, \quad Y=0,$

Ψ_n and T_n match with inner solution. (19c)

The solutions to the energy equations for T_0 and T_1 are

$$T_0 = H_0(\Psi_0) \tag{20a}$$

$$T_1 = H_1(\Psi_0)+\Psi_1 H_0'(\Psi_0). \tag{20b}$$

The equation (20a) shows that the temperature T_0 remains constant along the streamline Ψ_0. As there is no temperature gradient in the ambient environment, it follows from boundary condition (19) that $H_0 = 0$, thereby $T_0(X, Y) = 0$ for all X and Y. Based on the above argument and the fact that ambient environment is uniform, independent of Rayleigh number, it follows that $T_1(X, Y) = 0$ for all X and Y. Hence by induction it is found that the solution to equation (17b) subject to the boundary conditions (19a) and (19b) is

$$T_n(X, Y) = 0 \quad \text{for} \quad n, X \text{ and } Y. \tag{21}$$

Therefore equation (17a) reduces to

$$\nabla^2\Psi_n = 0 \tag{22}$$

for all n, the Laplace equation. As shown later the solution for lowest-order outer flow corresponds to ambient environment.

A thermal boundary layer is required to describe the flow in the plume. An order of magnitude analysis where convective and conductive heat transfer are of the same order leads to the following boundary-layer (inner) variables

$$\begin{aligned} &x = X, \quad y = Y/\lambda \\ &\psi(x, y) = \Psi(X, Y)/\lambda, \quad t(x, y) = T(X, Y) \end{aligned} \tag{23}$$

and an inner limit may be defined as y, ψ fixed for $\lambda\to 0$. In terms of inner variables, the equations (1) and (2) become

$$\psi_{yy} = t_y - \lambda^2\psi_{xx} \tag{24}$$

$$\psi_y t_x - \psi_x t_y = t_{yy} - \lambda^2 t_{xx}. \tag{25}$$

The boundary conditions at the axis of plume are

$$x>0, \quad y=0, \quad \psi = \psi_{yy} = t_y = 0 \tag{26a,b}$$

subject to heat flux relation

$$\int_{-\infty}^{\infty}\psi_y t \, dy = 1-\lambda^2\int_{-\infty}^{\infty} t_x \, dy. \tag{27}$$

The inner expansions for ψ and t can be taken as

$$\Psi = \Psi_0(x, y)+\lambda\psi_1(x, y)+\lambda^2\psi_2(x, y) + \lambda^3\psi_3(x, y)+\cdots+\lambda^{\alpha_m}\tilde{\psi}_m(x, y)+\ldots \tag{28a}$$

$$t = t_0(x, y)+\lambda t_1(x, y)+\lambda^2 t_2(x, y) + \lambda^3 t_3(x, y)+\cdots+\lambda^{\alpha_m}\tilde{t}_m(x, y)+\ldots \tag{28b}$$

where $\tilde{\psi}_m$ and $\tilde{t}_m$ are the eigensolutions associated with the problem and α_ms are the corresponding eigenvalues. Substituting the inner expansions (28) in inner equations (24)–(27) we get various order equations for ψ_n and t_n as

$$\psi_{n,yy} = t_{n,y} - a_{n-2}\psi_{n-2,xx} \tag{29}$$

$$\psi_{0,y}t_{n,x}-\psi_{0,x}t_{n,y} = t_{n,yy} - a_{n-1}\sum_{j=0}^{n-1} \times(\psi_{n-j+1,y}t_{j,x}-\psi_{n-j+1,x}t_{j,y})+a_{n-2}\nabla^2 T_{n-2} \tag{30}$$

$$x>0, \quad y=0; \quad \psi_n = \psi_{n,yy} = t_{n,y} = 0 \tag{31a,b,c}$$

$$\int_{-\infty}^{\infty}\psi_{0,y}t_n \, dy = 1-a_{n-1}\sum_{j}^{n-a}\int_{-\infty}^{\infty}\psi_{n-j+1,y}t_j \, dy - a_{n-2}\int_{-\infty}^{\infty} t_{n-2,x} \, dy. \tag{32}$$

The missing boundary condition for the inner layer at the edge of the plume is determined by matching inner and outer expansions. The matching of stream function gives

$$\Psi_0(X, 0) = 0 \tag{33}$$

$$\psi_0 \sim \Psi_1(X, 0)+y\Psi_{0,y}(X, 0), \quad y\to\infty \tag{34a}$$

$$\psi_1 \sim \Psi_2(X, 0)+y\Psi_{1,Y}(X, 0) + \tfrac{1}{2}y^2\Psi_{0,YY}(X, 0), \quad y\to\infty \tag{34b}$$

$$\psi_2 \sim \Psi_3(X, 0)+y\Psi_{2,y}(X, 0) + \tfrac{1}{2}y^2\Psi_{1,YY}(X, 0)+\tfrac{1}{6}y^3\Psi_{0,YYY}(X, 0), \quad y\to\infty \tag{34c}$$

and for temperature leads to

$$t_n(x, \infty) = 0 \quad \text{for all } n. \tag{35}$$

The equations governing the eigensolution $(\tilde{\psi}_m, \tilde{t}_m)$ are associated with homogeneous equations

$$\tilde{\psi}_{m,yy} = \tilde{t}_{m,y} \tag{36}$$

$$\psi_{0,y}\tilde{t}_{m,x}-\psi_{0,x}\tilde{t}_{m,y}+\tilde{\psi}_{m,y}t_{0,x}-\tilde{\psi}_{m,x}t_{0,y} = t_{m,yy} \tag{37}$$

subject to homogeneous boundary conditions

$$x>0; \quad y=0, \quad \tilde{\psi}_m = \tilde{\psi}_{m,yy} = \tilde{t}_{m,y} = 0 \tag{38a,b,c}$$

$$y \to \infty, \quad \tilde{\psi}_{m,y} = \tilde{t}_m = 0 \tag{38d,e}$$

$$\int_{-\infty}^{\infty} \psi_{0,y}\tilde{t}_m + \tilde{\psi}_{m,y} t_0 \, dy = 0 \tag{39}$$

(a) First-order boundary layer and eigensolutions

The solution to the lowest-order ($n = 0$) outer equation (22) for stream function Ψ_0 subject to boundary condition (19a) and (19b) and matching condition (33) is

$$\Psi_0(X, Y) = 0 \quad \text{for all} \quad X \text{ and } Y. \tag{40}$$

In the inner layer the first-order boundary-layer equations (29)–(32) with $n = 0$ under the transformation

$$\psi_0 = x^{1/3} f_0(\eta), \quad t_0 = x^{-1/3} h_0(\eta), \quad \eta = y/x^{2/3} \tag{41}$$

reduce to the following ordinary differential equations

$$f_0'' = h_0' \tag{42}$$

$$h_0'' + 1/3(f_0 h_0)' = 0. \tag{43}$$

The boundary and matching conditions are

$$f_0(0) = f_0''(0) = h_0'(0) = 0 \tag{44a,b,c}$$

$$f_0'(\infty) = h_0(\infty) = 0 \tag{44d,e}$$

subject to the normalization condition

$$\int_{-\infty}^{\infty} f_0' h_0 \, d\eta = 1. \tag{45}$$

Following Wooding [3] and Yih [4] the closed-form solution to first-order boundary-layer equations is obtained as

$$f_0(\eta) = A_0 \tanh(\eta A_0/6) \tag{46a}$$

$$h_0(\eta) = B_0 \operatorname{sech}^2(\eta A_0/6) \tag{46b}$$

where A_0 and B_0 are given by

$$A_0 = (9/2)^{1/3} \quad B_0 = (3/32)^{1/3}. \tag{47}$$

Before considering the higher-order terms in the asymptotic expansions it is appropriate to first analyse the eigensolution associated with the equations. Introducing the following variables

$$\tilde{\psi}_m = x^{(1-\alpha_m)/3} F_m(\eta) \tag{48a}$$

$$\tilde{t}_m = x^{-(1+\alpha_m)/3} H_m(\eta) \tag{48b}$$

the equations (36)–(39) governing the eigensolution reduce to

$$F_m''' = H_m' \tag{49}$$

$$H_m'' + \tfrac{1}{3} f_0 H_m' + (1+\alpha_m) f_0' H_m + F_m' h_0 + (1-\alpha_m) F_m h_0' = 0 \tag{50}$$

$$F_m(0) = F_m''(0) = H_m'(0) = F_m'(\infty) = H_m(\infty) = 0 \tag{51}$$

$$\int_{-\infty}^{\infty} F_m' h_0 + f_0' H_m \, d\eta = 0. \tag{52}$$

The first eigenvalue is $\alpha_1 = 3$ and the eigensolution is

$$F_1 = C(2\eta f_0' - f_0) \tag{53a}$$

$$H_1 = C(2\eta h_0' + h_0) \tag{53b}$$

where C is an unspecified multiplicative constant. It may be seen that the first eigensolution is proportional to partial differential of first-order equations (41) with respect to the x coordinate. It physically represents the uncertainty about the details of the flow near the heat source and arises from the fact that the initial conditions are not imposed on the similarity solution. As the first eigenvalue is $\alpha_1 = 3$, the eigensolution of the order of λ^3, is a higher-order effect associated with fourth-order terms in inner asymptotic expansions.

In the outer layer the eigenfunction $\tilde{\Psi}_m$ governed by

$$\nabla^2 \tilde{\Psi}_m = 0 \tag{54}$$

subject to homogeneous boundary conditions

$$\tilde{\Psi}_m = 0 \quad \text{at} \quad \theta = 0 \quad \text{and} \quad \beta \quad \text{or} \quad -\beta$$

yield the following eigensolution

$$\tilde{W}_m = \tilde{\Phi}_m + i\tilde{\Psi}_m = b_m Z^{-m\pi/\beta}, \quad m = 1, 2, 3 \tag{55}$$

representing the mass multipoles in the complex $Z = X + iY$ plane. As the reference length L is artificial, $\tilde{\Psi}_m$ is independent of L if we adopt

$$k_m = 3m\pi/\beta + 2 \tag{56}$$

and the first eigensolution in the outer layer occurs with the terms of order λ^5 for a free plume.

(b) Second-order boundary layer

The second-order outer flow is governed by

$$\nabla^2 \Psi_1 = 0 \tag{57}$$

The matching condition of the second-order outer flow Ψ_1 with the first-order boundary layer expressed by relation (34a) gives

$$X > 0, \quad Y = 0; \quad \Psi_1 = \lim_{y \to \infty} (\psi_0 - y\psi_{0y}) = A_0 X^{1/3}. \tag{58a}$$

The boundary conditions of the confined plume are

$$\theta = \beta \text{ or } -\beta, \quad \Psi_1 = 0 \tag{58b}$$

$$-\beta < \theta < \beta, \quad X^2 + Y^2 \to \infty, \quad \frac{\partial \Psi_1}{\partial Y} = 0. \tag{58c}$$

The solution to equations (57) and (58) in terms of complex potential $W_1(Z) = \Phi_1 + i\Psi_1$ as a function of complex variable $Z = X + iY$ is given by

$$W_1 = (C_R + iC_I) Z^{1/3} \tag{59}$$

where C_R and C_I are the real constant found from boundary conditions on Ψ_1 for $\arg Z \to 0$ and $\arg Z \to \beta$ as

$$C_I = A_0, \quad C_R = A_0 \cot \frac{\beta}{3}. \tag{60}$$

The solution to the confined plume is given by

$$W_1 = A_0\left(\mathrm{i}-\cot\frac{\beta}{3}\right)Z^{1/3}. \tag{61}$$

The complex velocity is

$$U_1-\mathrm{i}V_1 = \mathrm{d}W_1/\mathrm{d}Z = 1/3A_0\left(\mathrm{i}-\cot\frac{\beta}{3}\right)Z^{-2/3} \tag{62}$$

and the vertical velocity component at the axis of plume is

$$U_1(x,0) = -\frac{1}{3}A_0\cot\frac{\beta}{3}x^{-2/3}. \tag{63}$$

The special case of $\beta = \pi$ corresponds to a plume emerging in an unbounded media and the case $\beta = \pi/2$ to a plume emerging from a plane horizontal boundary.

The second-order boundary-layer equations (29)–(32) for $n = 1$, under the transformation

$$\psi_1 = f_1(\eta), \quad t_1 = x^{-2/3}h_1(\eta) \tag{64}$$

reduce to the following ordinary differential equations

$$f_1'' = h_1' \tag{65}$$

$$h_1''+\tfrac{1}{3}(f_0h_1'+2f_0'h_1+f_1'h_0) = 0. \tag{66}$$

The boundary conditions at the axis of plume are

$$f_1(0) = f_1''(0) = h_1'(0). \tag{67a,b,c}$$

The matching conditions (34b) and (35) require

$$\eta\to\infty, \quad f_1 \sim -\frac{A_0}{3}\cot\left(\frac{\beta}{3}\right)\eta + A_1, \quad h_1\to 0 \tag{67d,e}$$

subject to the heat flux relation

$$\int_{-\infty}^{\infty} f_1'h_0+f_0'h_1\,\mathrm{d}\eta = 0. \tag{68}$$

The closed-form solution to the first-order boundary-layer equations (65)–(68) is

$$f_1 = \frac{f_1'(\infty)}{2f_0'(0)}[2\eta f_0'(0)-\eta f_0'-f_0] \tag{69}$$

$$g_1 = -\frac{f_1'(\infty)}{2f_0'(0)}[\eta f_0''+2f_0']. \tag{70}$$

The velocity and temperature at the centreline of the plume are

$$f_1'(0) = 0 \tag{71a}$$

$$g_1(0) = -f_1'(\infty) = \frac{A_0}{3}\cot\left(\frac{\beta}{3}\right). \tag{71b}$$

Further, the constant A_1 in equation (67d) may be estimated from solution as

$$A_1 = \cot\left(\frac{\beta}{3}\right) \tag{72}$$

(*c*) *Third-order boundary layer*

The third-order outer flow is governed by the equation

$$\nabla^2\Psi_2 = 0. \tag{73}$$

The matching condition (34c) with the help of relations (64) and (67d) becomes

$$\Psi_2(X>0;\quad Y=0) = \lim_{y\to\infty}(\psi_1-y\psi_{1,y}-\tfrac{1}{2}y^2\psi_{1,yy}) = A_1. \tag{74a}$$

The boundary conditions for the confined plume are

$$\theta = \pm\beta, \quad \Psi_2 = 0 \tag{74b}$$

$$-\beta<\theta<\beta, \quad X^2+Y^2\to\infty, \quad \frac{\partial\Psi_1}{\partial Y} = 0. \tag{74c}$$

The solution to the third-order outer problem in terms of complex potential $W_2 = \Phi_2+\mathrm{i}\Psi_2$ is given by

$$W_2 = -\frac{A_1}{\beta}(\ln Z-\mathrm{i}\beta) \tag{75}$$

which signifies the sink flow towards the origin. The second-order complex velocity is given by

$$U_2-\mathrm{i}V_2 = \frac{\mathrm{d}W_2}{\mathrm{d}Z} = -\frac{A_1}{\beta Z} \tag{76}$$

and the third-order normal velocity at the axis of the plume is given by

$$U_2(x,0) = -\frac{A_1}{\beta X}. \tag{77}$$

The third-order boundary-layer equations (29)–(32) with $n = 2$, in terms of similarity variables

$$\psi_2 = x^{-1/3}f_2(\eta), \quad t_2 = x^{-1}h_2(\eta) \tag{78}$$

yield the following ordinary differential equations

$$f_2'' = h_2'+\tfrac{2}{9}(f_0-3\eta f_0'-2\eta^2f_0'') \tag{79}$$

$$h_2''+\tfrac{1}{3}(f_0h_3'+3f_0'h_2-f_2h_0'+f_2'h_0) = -\tfrac{2}{3}f_1'h_1-\tfrac{2}{9}(2h_0+7\eta h_0'+2\eta^2h_0''), \tag{80}$$

The boundary conditions at the axis are

$$f_2(0) = f_2''(0) = h_2'(0) = 0. \tag{81a,b,c}$$

The matching condition (34c) and (35) based on (61) and (75) require

$$\eta\to\infty, \quad f_2 \sim \frac{1}{9}A_0\eta^2-\frac{A_1}{\beta}\eta+A_2, \quad h_2\to 0 \tag{81d,e}$$

subject to integral heat flux relation

$$\int_{-\infty}^{\infty} f_2'h_0+f_1'h_1+f_0'h_2+\tfrac{1}{3}(h_0+2\eta h_0')\,\mathrm{d}\eta = 0. \tag{82}$$

(*d*) *Fourth-order boundary layer and eigensolution*

The fourth-order outer flow is governed by the relation

$$\nabla^2\Psi_3 = 0. \tag{83}$$

The matching relation (34c) with the third-order boundary layer gives

$$\Psi_3(X,0) = \lim_{y\to\infty}(\psi_2 - y\psi_{2y} - \tfrac{1}{2}y^2\psi_{2,yy}) = A_2X^{-1/3}. \quad (84)$$

The boundary conditions for the confined plume are

$$\theta = \pm\beta, \quad \Psi_3 = 0 \quad (84b)$$

$$-\beta < \theta < \beta, \quad X^2+Y^2\to\infty, \quad \frac{\partial\Psi_3}{\partial Y} = 0. \quad (84c)$$

The solution to the problem in terms of complex potential $W_3 = \Phi_3 + i\Psi_3$ is

$$W_3 = A_2\left(i+\cot\frac{\beta}{3}\right)Z^{-1/3} \quad (85)$$

and the vertical component of velocity at the axis of plume is

$$U_3(X,0) = -\frac{A_2}{3}\cot\left(\frac{\beta}{3}\right)X^{-2/3}. \quad (86)$$

In the inner layer, introducing the variables

$$\psi_3 = x^{-2/3}f_3(\eta), \quad t_3 = x^{-4/3}h_3(\eta) \quad (87)$$

the equations (29)–(32) with $n = 2$ reduce to ordinary differential equations. However, an inconsistency in the solution to the problem for (f_3, h_3) arises in the large behaviour as the first eigensolution described in section is of the same order as λ^3. This inconsistency can be resolved by introducing a log term in the inner asymptotic expansions. Therefore, the term $\lambda^3\psi_3$ and $\lambda^3 t_3$ in the expansions should be replaced by

$$\lambda^3x^{-2/3}\ln(\lambda x^{1/3})F_1(\eta) + \lambda^3x^{-2/3}f_3(\eta) \quad (88)$$

$$\lambda^3x^{-2/3}\ln(\lambda x^{-1/3})H_1(\eta) + \lambda^3x^{-2/3}h_3(\eta) \quad (89)$$

where (F_1, H_1) is the first eigensolution given by equations (53a,b) involving a multiplicative constant C. Accordingly the problem for (f_3, h_3) is modified to include the addition terms that are mutiplied by C. The constant C may be determined for proper asymptotic behaviour of the solution of (f_3, h_3) for large η. Finally, however, in the solution for (f_3, h_3) another constant that is associated with the complementary solution of the problem is left unspecified. Furthermore, for computational purposes the two terms in (88) are to be treated together. There is no unique way of fixing this constant unless measurements are available, the analysis is not pursued further.

3. RESULTS AND DISCUSSION

The higher-order effects for Darcian free convection, about a horizontal line source of heat, emerging from the apex of a symmetrical (insulated) wedge with its axis coinciding with the direction of the buoyant force vector is studied by the method of matched asymptotic expansions. From the analysis presented earlier the inner asymptotic expansions may be summarized as

$$\Psi_* = U\delta f(\varepsilon,\eta), \quad T_* - T_{*\infty} = \frac{Q}{U\delta}h(\varepsilon,\eta) \quad (90)$$

$$f(\varepsilon,\eta) = f_0(\eta)+\varepsilon f_1(\eta)+\varepsilon^2 f_2(\eta) + \varepsilon^3\ln\varepsilon F_1(\eta)+\varepsilon^3 f_3(\eta)+\cdots \quad (91a)$$

$$h(\varepsilon,\eta) = h_0(\eta)+\varepsilon h_1(\eta)+\varepsilon^2 h_2(\eta) + \varepsilon^3\ln\varepsilon H_1(\eta)+\varepsilon^3 h_3(\eta)+\cdots \quad (91b)$$

$$\eta = Y_*/\delta \quad (92)$$

where

$$\delta = \varepsilon X_* \quad U = \alpha/(\varepsilon^2 X_*) \quad (93)$$

$$\varepsilon = Ra_x^{-1/3} \quad (94)$$

and Ra_x is the local Rayleigh number defined as

$$Ra_x = \frac{Qg\gamma KX_*}{\rho C_p\nu\alpha^2}. \quad (95)$$

The outer expansions for complex potential $W(Z_*) = \Phi_* + i\Psi_*$, $Z_* = X_* + iY_*$ and temperature can be summarised as

$$W(Z_*) = \alpha\,\mathrm{cosec}\,(\beta/3)[-A_0\hat{Z}^{1/3} - A_1\beta^{-1}\sin(\beta/3)\ln\hat{Z} + A_2\hat{Z}^{-1/3} + \hat{Z}^{-2/3}(A_3\ln\hat{Z}+A_3)+\cdots] \quad (96)$$

$$T_* - T_{*\infty} \simeq 0 \quad (97)$$

where

$$\hat{Z} = \frac{g\beta QK}{\rho C_p\nu\alpha^2}Z_*e^{-i\beta}. \quad (98)$$

The outer eigensolution complex potential

$$\bar{W}_m = b_mZ^{-m\pi/\beta}, \quad m = 1,2,3,\ldots, \quad (99)$$

representing mass multipoles in the Z-plane, leads to further log terms in the outer expansion (96).

The velocity components U_* and V_* in X_* and Y_* directions in the outer layer are related to the first differential of complex potential

$$U_* - iV_* = \frac{dW}{dZ_*}.$$

The vertical component of velocity from the outer solution at the axis of plume from equations (96) and (98) is given by

$$U_*(X_*,0) = \alpha\left[-\frac{A_0}{3}\cot\left(\frac{\beta}{3}\right)\varepsilon - \frac{A_1}{\beta}\varepsilon^2 - \frac{A_2}{3}\cot\left(\frac{\beta}{3}\right)\varepsilon^3 - \varepsilon^4\left\{\frac{2}{3}\tilde{A}_3\ln\varepsilon + \frac{2}{3}A_3 - \tilde{A}_3\right\}+\cdots\right] \quad (100)$$

The inner and outer expansions to the order ε^2, i.e. the third-order boundary layer has been studied.

The first-order boundary-layer equations, reducing to the equations for Schlichting's two-dimensional

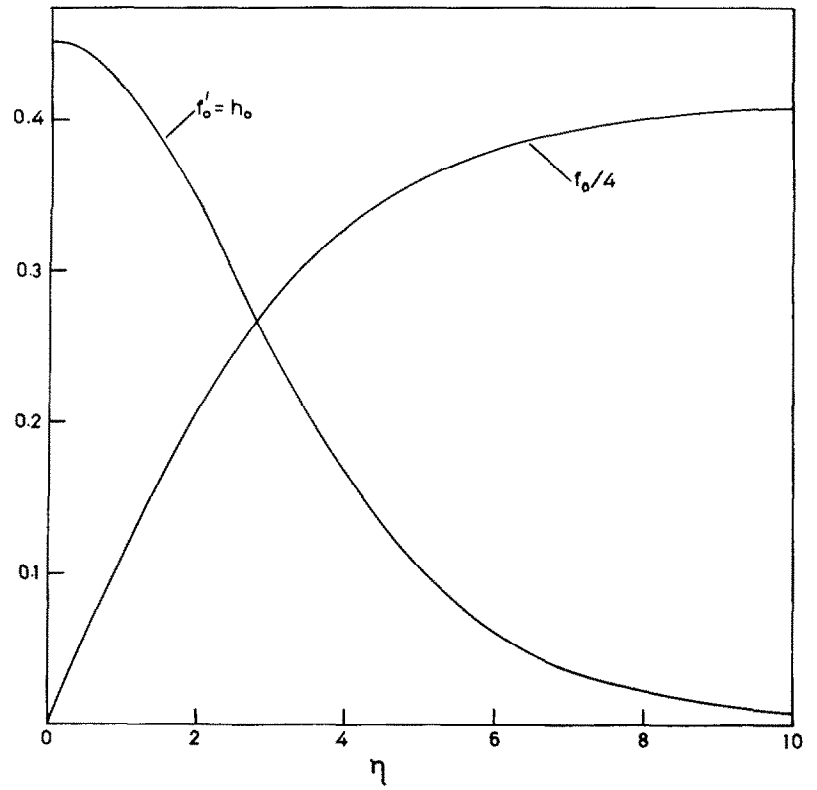

FIG. 2. First-order boundary layer: the velocity and temperature distributions in the plume.

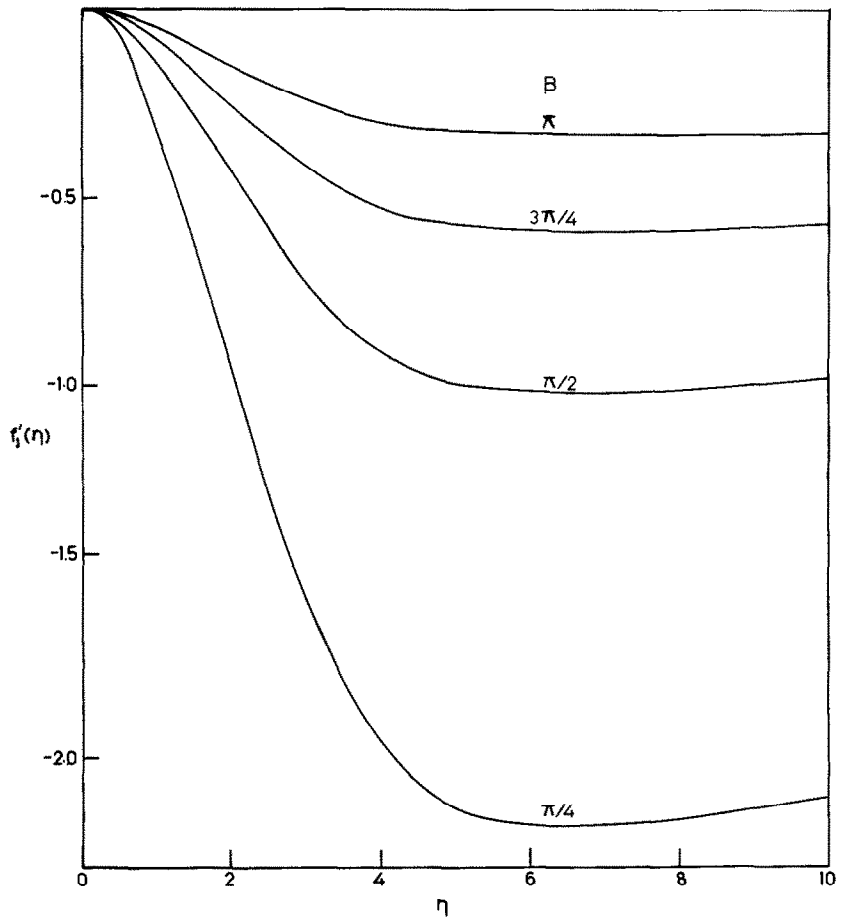

FIG. 3. Second-order boundary layer: second-order velocity distribution in the bounded plume for various values of wedge angles β.

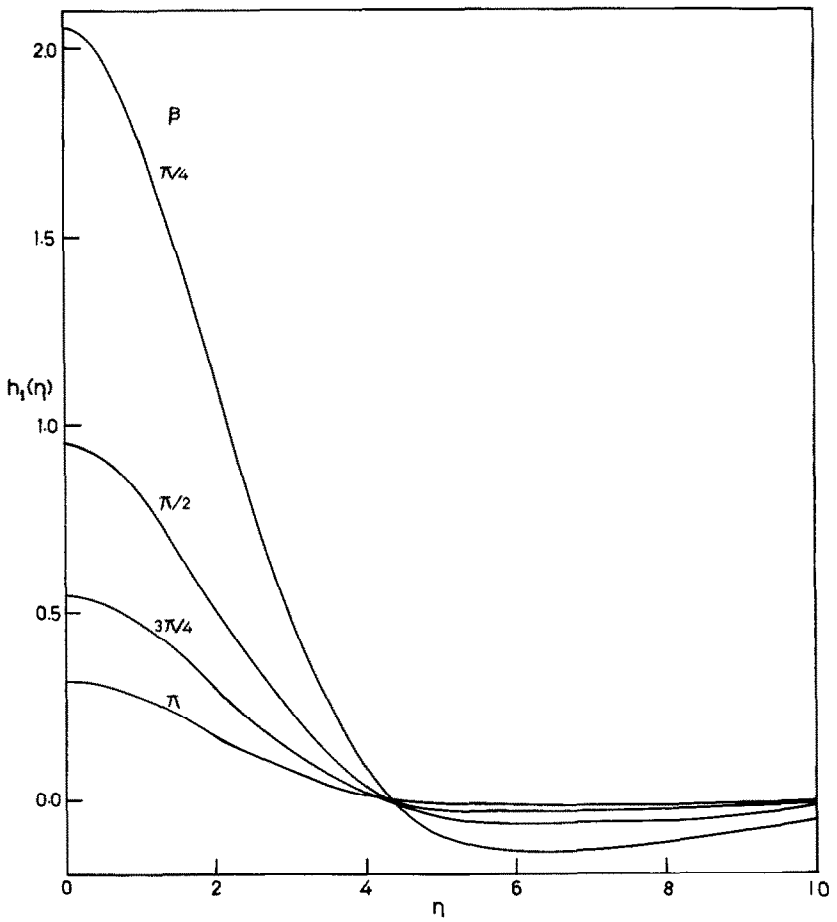

FIG. 4. Second-order boundary layer: second-order temperature distribution in the bounded plume for various values of wedge angles β.

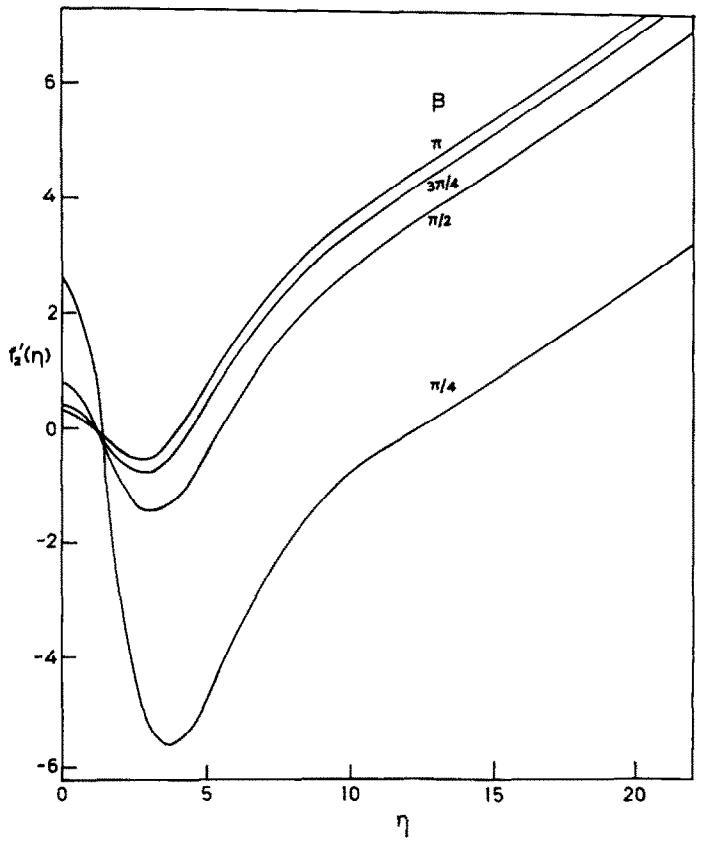

FIG. 5. Third-order boundary layer: third-order velocity distribution in the bounded plume for various values of wedge angles β.

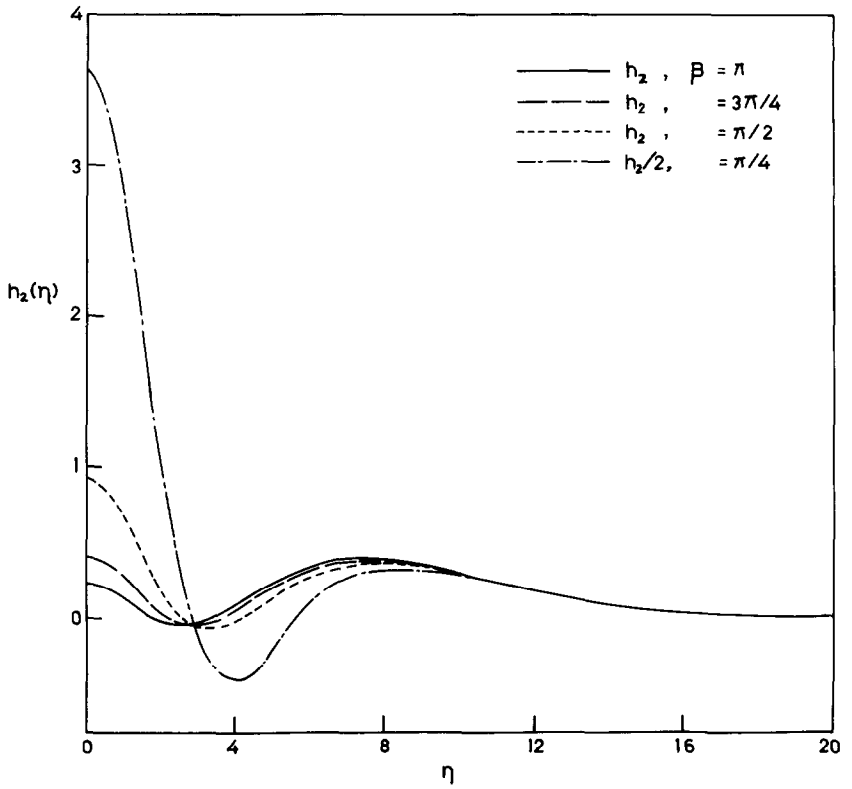

FIG. 6. Third-order boundary layer: third-order temperature distribution in the bounded plume for various values of wedge angles β.

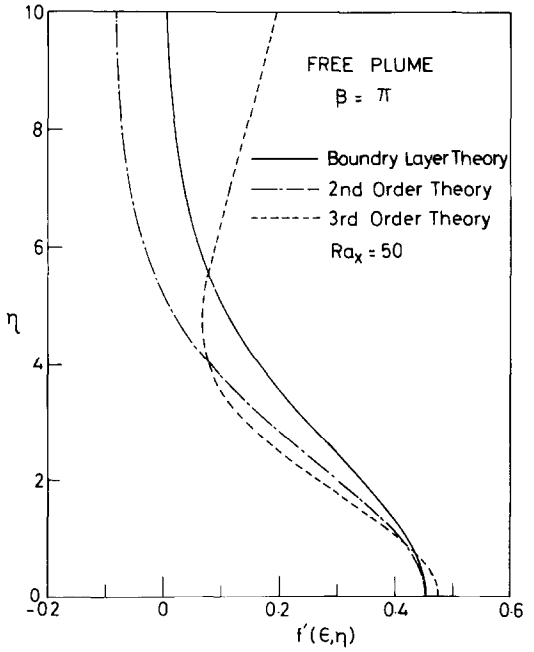

FIG. 7. Velocity distribution in the plume for unbounded media from first-, second- and third-order boundary-layer effects at local Rayleigh number of 50.

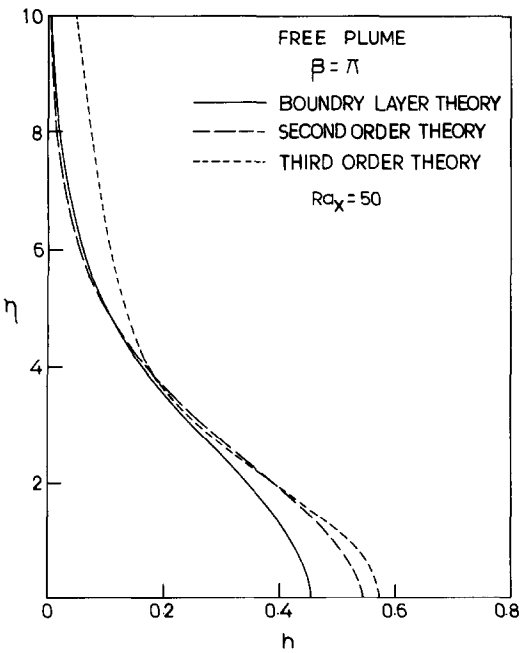

FIG. 8. Temperature distribution in the plume for unbounded media from first-, second- and third-order boundary-layer effects at local Rayleigh number of 50.

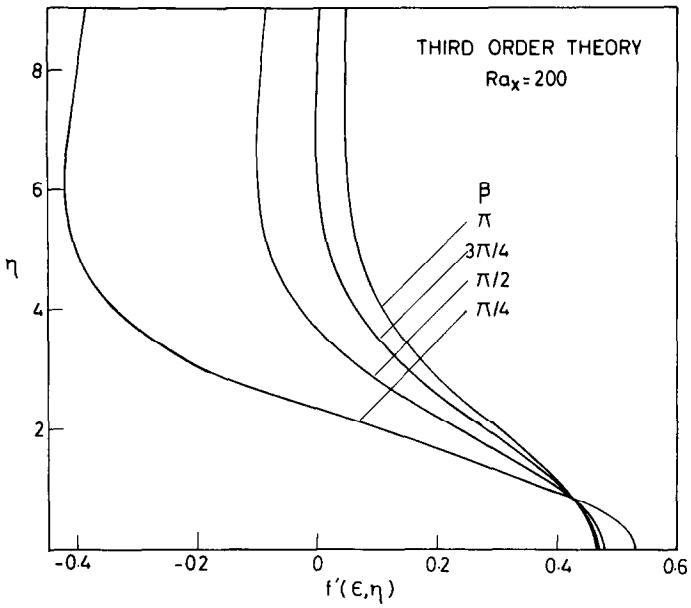

FIG. 9. Effects of wedge angle β on the total velocity distribution in the plume from third-order boundary-layer theory at $Ra_x = 200$.

laminar jet in a Newtonian fluid, are solved in closed form. The second-order boundary-layer equations, however, differ from the corresponding equations for laminar jet in a Newtonian fluid [11], are also solved in closed form for arbitrary values of β. The third-order boundary-layer equations have been integrated numerically for a free plume ($\beta = \pi$) and for a plume bounded by symmetric wedge with $\beta = 3\pi/4$, $\pi/2$ and $\pi/4$.

The velocity and temperature profiles for the first-order boundary layer displayed in Fig. 2 are independent of the fact of whether the plume is in unbounded or bounded medium. This is because at large Ra_x the first-order plume being very thin, like $Ra_x^{-1/3}$, is not affected by the confinement of the medium. At moderately large Ra_x, the plume becomes thicker, resulting in increased entrainment of fluid in the boundary layer from the outer irrotational domain and gives rise to the second-order corrections to the plume boundary layer. The entrainment depends on the extent of outer zone, i.e. whether the plume can entrain from entire or limited space. Therefore, the second-order boundary layer should also depend on the wedge angle bounding the plume; the velocity and

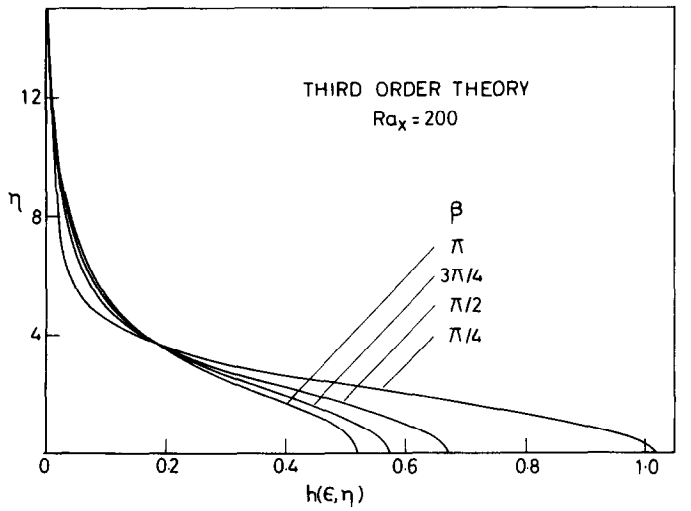

FIG. 10. Effects of wedge angle β on the total temperature distribution in the plume from third-order boundary-layer theory at $Ra_x = 200$.

Table 1. Characteristic values for two-dimensional buoyant plume bounded by symmetrical adiabatic wedge of included angle 2β from second- and third-order boundary-layer effects.

β	$f'_2(0)$	$h_1(0)$	$h_2(0)$	A_1	A_2	Remark
π	0.27040	0.31773	0.45418	0.57735	−3.55850	Free plume
$3\pi/4$	0.40382	0.55032	0.82824	1.0	−3.21150	
$\pi/2$	0.75120	0.95318	1.85386	1.73206	−2.03590	Plume bounded by horizontal surface
$\pi/4$	2.58043	2.05382	7.33225	3.73207	4.56289	

temperature profiles from the solution of the second-order boundary layer equations are displayed in Figs. 3 and 4 for $\beta = \pi$, $3\pi/4$, $\pi/2$ and $\pi/4$. The case $\beta = \pi$ corresponds to a free (unbounded) plume and $\beta = \pi/2$ to the plume emerging and bounded by horizontal surface. Figure 3 shows that at $\eta = 0, f'_1(\eta)$ is zero and for $\eta > 0$, $f'_1(\eta)$ is negative whereas Fig. 4 shows that $h_1(\eta)$ is positive near the axis of plume and becomes negative near the outer edge of plume. The effect of decrease of wedge angle β is to increase the magnitude of the second-order effects. Therefore, for a fixed angle, the second-order effects decrease the velocity in the plume, the exception being $\eta = 0$, whereas the temperature increases near the axis and decreases more rapidly towards the outer edge of the plume and the width of the plume becomes less extensive. For further moderate values of Ra_x the third-order boundary-layer effects become significant and the velocity and temperature profiles from numerical solutions for $\beta = \pi$, $3\pi/4$, $\pi/2$ and $\pi/4$ are displayed in Figs. 5 and 6. These figures show that for a fixed β, second-order velocity $f'_2(\eta)$ and temperature $h_2(\eta)$ are positive near the axis and towards the outer edge but in between the axis and the edge of the plume there is a domain where f'_2 and h_2 become negative. This implies that the third-order effect tends to increase the velocity and temperature near the axis and towards the outer edge and decrease it in a small domain between the axis and the edge of the plume. The effect of decrease of wedge angle β is also to increase the third-order effects.

For a free plume ($\beta = \pi$) the velocity and temperature distributions in the plume for $Ra_x = 50$ obtained from first-, second- and third-order boundary-layer solutions are displayed in Figs. 7 and 8, respectively. The effect of confinement of the plume for various values of β on total velocity and temperature distributions based on third-order effects are displayed in Figs. 9 and 10 which clearly display the nature of solutions depicted above.

At the centreline of the plume the velocity and temperature are given by

$$U_*(X,0) = U[0.45428 + f'_1(0)\varepsilon + f'_2(0)\varepsilon^2 + O(\varepsilon^2)] \tag{101}$$

$$T_*(x,0) - T_{*\infty} = \frac{Q}{U\delta}[0.45428 + h_1(0)\varepsilon + h_2(0)\varepsilon^2 + O(\varepsilon^2)] \tag{102}$$

where $f'_1(0) = 0$ and coefficients $f'_2(0), h_1(0)$ and $h_2(0)$ are given in Table 1 for various values of β. It may be seen that the higher-order effects for a given β increase the velocity and temperature at the axis of the plume, the increase being much more rapid as β decreases. In terms of mathematical order the higher-order analysis is valid for $\varepsilon \cot(\beta/3) \ll 1$. Physically, the higher-order theory breaks down if the magnitude of the subsequent term becomes comparable to previous term. As the decrease of β increases the magnitude of the second- and third-order coefficient in the series (101) and (102) it follows that in these cases, the value of ε where higher-order theory is valid also decreases. For example, series (101) and (102) yield useful estimates for free plume ($\beta = \pi$) when $\varepsilon \lesssim 0.8$, for plume bounded by horizontal wall ($\beta = \pi/2$) when $\varepsilon \lesssim 0.5$ and for confined plume with $\beta = \pi/4$ when $\varepsilon \lesssim 0.2$.

REFERENCES

1. M. A. Combarnous and S. A. Bories, Hydrothermal convection in saturated porous media. In *Advances in Hydroscience*, Vol. 10, pp. 231–307. Academic Press, New York (1975).
2. P. Cheng, Heat transfer in geothermal systems. In *Advances in Heat Transfer*, Vol. 14, pp. 1–105. Academic Press, New York (1978).
3. R. W. Wooding, Convection in a saturated porous medium at large Rayleigh or Peclet number, *J. Fluid Mech.* **15**, 527–544 (1963).
4. C. S. Yih, *Dynamics of Nonhomogeneous Fluids*. Macmillan, New York (1965).
5. M. Van Dyke, Higher order boundary layer theory, *Ann. Rev. Fluid Mech.* **1**, 269–292 (1969).
6. K. T. Yang and E. W. Jerger, First-order perturbations of laminar free convection boundary layer on a vertical plate, *J. Heat Transfer* **28**, 107–115 (1964).
7. N. Riley, Free convection from a horizontal line source of heat, *Z. angew. Math. Mech.* **25**, 817–828 (1974).
8. C. A. Hieber and E. J. Nash, Natural convection above a line heat source. Higher order effects and stability. *Int. J. Heat Mass Transfer* **18**, 1473–1479 (1975).
9. N. Afzal, Mixed convection in buoyant plumes. In *Handbook of Heat and Mass Transfer Operations* (Edited by N. P. Cheremissinof), Chap. 13, pp. 389–440. Gulf Publishing, Texas (1985).
10. I. D. Chang and P. Cheng, Matched asymptotic expansions for free convection about an impermeable horizontal surface in a porous medium. *Int. J. Heat Mass Transfer* **26**, 163–174 (1983).
11. S. G. Rubin and R. Falco, Plane laminar jet, *AIAA Jl.* **6**, 186–187 (1968).

PANACHE BIDIMENSIONNEL DANS UN MILIEU POREUX: EFFETS D'ORDRE ELEVE

Résumé—La convection naturelle à partir d'une source rectiligne horizontale de chaleur noyée dans un milieu poreux a été étudiée par la méthode des développements asymptotiques aux grands nombres de Rayleigh. Le cas général d'un panache confiné sortant du sommet d'un dièdre symétrique, avec son axe en coïncidence avec la direction du vecteur accélération de la pesanteur, est considéré pour des valeurs différentes d'angle du dièdre. Le problème du premier-ordre réduit à l'approximation de couche-limite considérée antérieurement par Wooding [*J. Fluid Mech.* **15**, 527–544 (1963)]. Pour les équations de couche limite de second ordre, représentant l'effet d'entrainement, une solution analytique est donnée et pour le troisième ordre, représentant les effets de la conduction thermique axiale et du gradient de pression, les équations sont intégrées numériquement. Les résultats sont donnés graphiquement et une discussion critique est menée.

ZWEIDIMENSIONALE AUFTRIEBSFAHNE IN PORÖSEN MEDIEN: EFFEKTE HÖHERER ORDNUNG

Zusammenfassung—Die natürliche Konvektion um eine zweidimensionale, horizontale, linienförmige, in ein poröses Medium eingebettete Wärmequelle wurde mit der Methode der asymptotischen Annäherung für große Rayleigh-Zahlen untersucht. Der allgemeine Fall einer begrenzten Auftriebsfahne, die vom Scheitelpunkt eines isolierten symmetrischen Keils aufsteigt, dessen Achse mit der Auftriebsrichtung übereinstimmt, wird für beliebige Keilwinkel untersucht. Das Problem erster Ordnung führt auf die Grenzschichtnäherung, die bereits früher von Wooding betrachtet worden ist [*J. Fluid Mech.* **15**, 527–544 (1963)]. Für die Grenzschichtgleichungen zweiter Ordnung, welche den Entrainment-Effekt berücksichtigen, wird eine Lösung in geschlossener Form angegeben, und für die Gleichungen dritter Ordnung, welche die axiale Wärmeleitung und den senkrechten Druckgradienten enthalten, werden die Gleichungen numerisch integriert. Die Ergebnisse werden grafisch dargestellt und kritisch diskutiert.

ДВУМЕРНАЯ ВОСХОДЯЩАЯ СВОБОДНО-КОНВЕКТИВНАЯ СТРУЯ В ПОРИСТЫХ СРЕДАХ. ЭФФЕКТЫ ВЫСОКОГО ПОРЯДКА

Аннотация—Методом сращиваемых асимптотических разложений при больших числах Рэлея исследуется естественная конвекция от двумерного горизонтального линейного источника тепла, погруженного в пористую среду. Общий случай ограниченной фонтанирующей среды, выходящей из вершины изолированного симметричного клина, ось которого совпадает с направлением вектора подъемной силы, рассматривается для произвольных значений угла клина. Задача первого порядка сводится к приближению пограничного слоя, ранее изучаемому Вудингом [*J. Fluid Mech.* **15**, 527–544 (1963)]. Для уравнений пограничного слоя второго порядка, определяющим эффект увлечения, дано решение в замкнутом виде, а уравнения третьего порядка, выражающие эффекты осевой теплопроводности и градиент нормального давления, интегрируются численно. Обсуждаемые результаты представлены графически.